Dependence of decaying homogeneous isotropic turbulence on initial conditions

P. C. VALENTE
J. C. VASSILICOS

Department of Aeronautics, Imperial College London, London SW7 2AZ, United Kingdom

(Received ?? and in revised form ??)

We conduct a careful analysis of the data provided by Krogstad & Davidson (2011) and show that their data do not support their conclusions. According to their published data, their decaying approximately homogeneous isotropic turbulent flows are, invariably, clearly different from Saffman turbulence; and very clearly marked differences exist between the far downstream turbulence behaviors generated by their conventional grid and by their multiscale cross grids.

1. Introduction

A few years ago, Lavoie, Djenidi & Antonia (2007) investigated potential effects of initial conditions on the decay of approximately homogeneous isotropic turbulence. Initial conditions refer to the way the turbulence is generated. In the wind tunnel experiments of these authors, the turbulence was passively generated by square-mesh biplane grids placed at the test section entry. A particular aspect of the potential dependence on initial conditions is whether the power-law decay of the far-downstream turbulence depends on them. Quantitatively, the question is whether the decay exponent n in

$$u^2 \sim (x - x_0)^{-n} \tag{1.1}$$

(where u^2 stands for two thirds of the turbulent kinetic energy and x is the streamwise distance along the tunnel, x_0 being a virtual origin) differs for different initial conditions as claimed by George (1992).

Lavoie *et al.* (2007) tried four different conventional passive grids (with square or with round bars with/without a small helical wire) and two different test sections (one with and one without a secondary contraction to improve isotropy). They did not find any significant effect of initial conditions on the decay exponent n other than that of anisotropy which does, itself, depend on initial conditions and persists far downstream.

Krogstad & Davidson (2011) carried out a similar wind tunnel study but with two multiscale grids and one conventional grid. Their grids were all monoplanar and their two multiscale grids were chosen from one of the three families of multiscale grids introduced by Hurst & Vassilicos (2007), specifically the family of fractal cross grids. These grids are very different from the low-blockage space-filling fractal square grids which have been the multiscale grids of choice in the vast majority of subsequent works on multiscale/fractal-generated turbulence (Seoud & Vassilicos 2007; Nagata, Suzuki, Sakai, Hayase & Kubo 2008*a*,*b*; Stresing, Peinke, Seoud & Vassilicos 2010; Mazellier & Vassilicos 2010; Suzuki, Nagata, Sakai & Ryota 2010; Laizet & Vassilicos 2011; Valente & Vassilicos 2011). The reason why multiscale/fractal cross grids have mostly been neglected (except in studies where they were used to enhance the Reynolds number, see Kinzel, Wolf, Holzner, Lüthi, Tropea & Kinzelbach (2010); Geipel, Henry Goh & Lindstedt (2010)) is that Hurst & Vassilicos (2007) did not make any strong or unexpected claim about the dependence of u^2 on $x - x_0$ in decaying

turbulence generated by them. Their conclusion on these grids was just a double negative: "the turbulence decay observed is not in disagreement with power-law fits and the principle of large eddies".

Sketches of the multiscale cross grids used by Krogstad & Davidson (2011) can be seen in their figure 1 and are described in their section 2 where they are labeled *msg1* and *msg2*. We do not need to repeat the description here except to say that each multiscale cross grid has three different mesh sizes, the smallest one being $M_3 = 15mm$ for *msg1* and $M_3 = 21mm$ for *msg2*. Krogstad & Davidson (2011) were careful to design their two multiscale cross grids and one conventional grid in such a way that the longitudinal integral length-scale of the turbulence at a 2m distance from the grid location is the same $\ell_0 \approx 23.65mm \pm 0.25mm$ for all three grids. The ratio between ℓ_0 and the distance between the tunnel walls is smaller than 1/75.

A description of the wind tunnel used by Krogstad & Davidson (2011) can be found in Krogstad & Davidson (2010, 2011). It is much larger and longer than the tunnel used by Hurst & Vassilicos (2007) and the grids were placed in the tunnel contraction, specifically 1.2m upstream from the start of their test section. As a result, the multiscale grid-generated turbulence of Krogstad & Davidson (2011) is more isotropic and much further downstream of the grid than in Hurst & Vassilicos (2007). Their turbulence measurements were taken using single and two component hot-wire anemometry from $x \approx 60\ell_0$ till $x = 400\ell_0$ which means $93M_3 \leqslant x \leqslant 629M_3$ for *msg1* and $67M_3 \leqslant x \leqslant 446M_3$ for *msg2*. This is clearly much further downstream than Hurst & Vassilicos (2007) who could not take measurements beyond a distance equal to 80 times the smallest mesh size of their own multiscale cross grids. In the case of Krogstad & Davidson (2011) conventional grid (refered to as *cg*), $60\ell_0 \leqslant x \leqslant 400\ell_0$ corresponds to $40M \leqslant x \leqslant 240M$ where M is the mesh size of the grid.

The first main conclusion of Krogstad & Davidson (2011) was that their "results are at odds" and that their "findings contradict" those of Hurst & Vassilicos (2007). This claim is factually incorrect not only because the multiscale cross grids in these two studies have significant differences (different blockages, but also differences in some other grid-defining parameters, see figure 1 in Krogstad & Davidson (2011) and figure 3 in Hurst & Vassilicos (2007) and related parameters), but also because the regions of the flow were different, in fact not even overlapping (if just barely in one case), in terms of multiples of the smallest mesh size of the multiscale cross grids. The fact that Hurst & Vassilicos (2007) measured higher turbulence levels and local Reynolds numbers $Re_\lambda = u\lambda/\nu$ (where λ is the Taylor microscale and ν the kinematic viscosity) than Krogstad & Davidson (2011) is quite simply consistent with the fact that Hurst & Vassilicos (2007) measured much closer to the grid. Hurst & Vassilicos (2007) also extracted decay exponents n from their data and showed how they vary continuously as the choice of virtual origin x_0 varies (see their figure 10). Choosing x_0 close to 0, they found exponents n close to 1.2 for their multiscale cross grids and close to 1.4 for their conventional grid with large mesh size. However, they also proposed a λ-based method for choosing x_0 which returned $n \approx 1.75$ for their multiscale cross grids, $n \approx 2.3$ for their conventional grid with high mesh size and $n \approx 1.39$ for their conventional grid with usual mesh size. These particular λ-based exponents are indeed higher than those claimed by Krogstad & Davidson (2011) which lie between 1.12 and 1.25 but they were obtained in completely different regions of the flow and, most importantly, with different fitting methods which yielded very different values of x_0. In fact Hurst & Vassilicos (2007) did not include these exponents in their conclusions because "more extensive checks of large-scale and small-scale isotropy as well as homogeneity will be required to fully conclude on the nature of the turbulence decay

behind fractal cross grids, in particular in order to assess the viability of our λ-based method for estimating x_0 in the cross grid-generated flows".

The second main conclusion of Krogstad & Davidson (2011) is that, in the far-region where they measure, their multiscale cross grids and their conventional grid produce "virtually identical" turbulence behavior. Furthermore, quoting from their conclusion, "Saffman's decay law is reasonably robust, since the energy decay exponents for all three grids are close to Saffman's classical prediction of $n = 6/5$". In the next two sections we use the data published by Krogstad & Davidson (2011) and show that an attentive analysis of their data based on Krogstad & Davidson (2010) leads to very different conclusions.

2. Decaying homogeneous isotropic turbulence with three different initial conditions

Krogstad & Davidson (2011) established that their turbulent flows were reasonably homogeneous at x beyond $2m$ in terms of longitudinal profiles of variances, skewnesses and flatnesses of the streamwise fluctuating velocity component. Their centreline mean streamwise flow U remains constant to within less than $\pm 0.1\%$ for all three grids from $x = 2m$ till about $x = 8m$, though it deviates a very little bit for *msg2* beyond $x = 6.5m$. As a result, they chose to design their three grids in such a way that they all generate turbulence with nearly same longitudinal integral length-scale ℓ_0 at $x = 2m$. The positions $x = 80\ell_0$ fall around $1.9m$ for all the grids. (Krogstad & Davidson (2011) in fact recorded, and in a few instances used for their analysis, a few measurements at closer distances to the grid, i.e. x as small as about $41\ell_0$.) The longitudinal length-scale ℓ grows as the turbulence moves downstream, but the ratio between ℓ and the distance between the tunnel walls remains very small, for example less than about $1/40$ at about $8m$ from the grid location.

They also calculated ratios $< u_x^2 > / < u_y^2 >$, $< u_x^2 > / < u_z^2 >$ and $u^2 / < u_x^2 >$ and found small levels of anisotropy "comparable, if not better, than in most other experiments". In particular, $u^2 / < u_x^2 >$ hovers between 0.95 and 1.02 throughout the regions where they recorded their measurements. Hence any anisotropy-related dependence on initial conditions as in Lavoie *et al.* (2007) can, most probably, be ruled out.

In figure 1a we plot $< u_x^2 > /U^2$ versus $(x - x_0)/\ell_0$ for all three grids as well as fits of the data by $< u_x^2 > /U^2 \sim (\frac{x-x_0}{\ell_0})^{-n}$. The decay exponents n and virtual origins x_0 in these fits are estimated simultaneously by direct application of a non-linear least-squares regression algorithm ('NLINFIT' routine in MATLAB^{TM}). This fitting method is closely related to the one used by Lavoie *et al.* (2007) and we apply it to nearly the same range where Krogstad & Davidson (2011) applied their own fitting methods. Specifically, we apply our fit to the range $80\ell_0 < x < 330\ell_0$ which is a range of x from about $1.9m$ to $8m$. This means that, for each grid, we exclude data points obtained by Krogstad & Davidson (2011) at values of x smaller than $80\ell_0$ where according to these authors the turbulence is not sufficiently homogeneous, and we also exclude, exactly like Krogstad & Davidson (2011) do, the data points furthest downstream where noise starts to be significant. (Including data points from $x \approx 1.5m$ (i.e. $60\ell_0$) as in Krogstad & Davidson (2011) makes little difference as the values of n remain the same to within ± 0.01.)

We give the values of n and x_0 thus obtained in table 1 (method I). These values agree fairly well with the various values of n and x_0 obtained by Krogstad & Davidson (2011) by their three different fitting methods for all three grids except for their value of x_0 for *msg1* and their value of n for *msg1* when they use one of their three fitting methods, the

regression method (see their table 1). The values of n which they obtain for *msg1* with their other two fitting methods are close to our value of n for *msg1*.

At this point it may be helpful to recall some basic theoretical considerations. Homogeneous turbulence in the wind tunnel decays according to $U\frac{d}{dx}\frac{3}{2}u^2 = -\epsilon$ where ϵ is the turbulent kinetic energy dissipation per unit mass. To obtain (1.1) and the numerical value of n, one needs some more information about u^2 and ϵ. This information usually consists of the following three ingredients when the homogeneous turbulence can also be considered fairly isotropic (see Batchelor & Townsend 1948; Batchelor 1953; Rotta 1972): (i) a finite invariant of the von Kárman-Howarth equation, (ii) the assumption that the decay of large eddies is self-similar and (iii) the empirical assumption that

$$A \equiv \epsilon\ell/u^3 \tag{2.1}$$

remains constant during decay ($\ell = \ell(x)$ is the longitudinal integral length-scale). This constancy can be thought of as resulting from the assumed independence of A on turbulence intensity and Re_λ.

Vassilicos (2011) proved that there are four different cases of finite invariants of the von Kárman-Howarth equation depending on conditions at infinity. A case where no known finite invariant exists; a case where the Loitsyansky invariant is the only known finite invariant and where self-similar decay of large eddies implies $u^2\ell^5 = const$ during decay; a case where only one known finite invariant exists and where self-similar decay of large eddies implies $u^2\ell^{m+1} = const$ with $2 \leqslant m < 4$ ($2 \leqslant m$ ensures that the spectral tensor does not diverge at zero wavenumber as stated in Rotta (1972), in the Appendix of Krogstad & Davidson (2011) and in Vassilicos (2011)); and a case where two finite invariants exist and where, as a consequence, self-similar decay of large-eddies is impossible.

Using the constancies of A and $u^2\ell^{m+1}$, the second and third of these four cases imply

$$n = 2(m+1)/(m+3) \tag{2.2}$$

where $2 \leqslant m \leqslant 4$ and therefore $6/5 \leqslant n \leqslant 10/7$. There is no known way to rule out the first and fourth cases and therefore no known theoretical reason for measured values of n to necessarily lie inside the range $6/5 \leqslant n \leqslant 10/7$.

Two out of the three present grids have returned values of n which are below $6/5 = 1.2$ (see table 1 under method I). However, this does not imply that the present turbulence measurements do not fall under the second or third cases identified by Vassilicos (2011). Indeed, as Krogstad & Davidson (2010, 2011) have observed, A varies slowly with x and is therefore not strictly constant. If this is so, then (2.2) needs to change.

In figure 2 we plot the values of A obtained by Krogstad & Davidson (2011) for their three grids as functions of $(x - x_0)/\ell_0$ where x_0 is taken from table 1 (method I). (Krogstad & Davidson (2011) assumed small-scale isotropy and calculated A from measurements of $< (\frac{\partial u_x}{\partial x})^2 >$ using $\epsilon = 15\nu < (\frac{\partial u_x}{\partial x})^2 >$ and integrations of measured longitudinal correlation functions to educe ℓ.) To bring out more clearly the differences between grids we in fact plot A/A_1 where A_1 is the value of A obtained at the smallest distance x from each grid. We then follow Krogstad & Davidson (2010) and fit the power law $A \sim (\frac{x-x_0}{\ell_0})^{-p}$ in the range $60\ell_0 < x < 330\ell_0$ of this data. These fits are shown in figure 2 and the values of p are reported in table 1.

If $A = const$ is replaced by $A \sim (x - x_0)^{-p}$ then the implication of $u^2\ell^{m+1} = const$ changes from (2.2) to

$$n = (1-p)2(m+1)/(m+3) \tag{2.3}$$

where $2 \leqslant m \leqslant 4$. With our estimates of n and p we can now use (2.3) to derive values of

m for each grid. They are given in table 1 (under method I) and, having now taken into account the slight variations of A, they are all between 2 and 4. Similarly, the values of $n_{corr} \equiv n/(1-p)$ lie all between 6/5 and 10/7 (see table 1 under method I).

These values of m raise the possibility that the three decaying nearly homogeneous and nearly isotropic turbulent flows of Krogstad & Davidson (2011) may be three different instances of the third case identified by Vassilicos (2011) where only one known finite invariant exists and where self-similar decay of large eddies implies $u^2\ell^{m+1} = const$ with $2 \leqslant m < 4$. The Saffman invariant corresponds to $m = 2$ but none of the grids used by Krogstad & Davidson (2011) returns such a value of m. In figure 3a we plot $< u_x^2 > \ell^{m+1}/(U^2\ell_0^{m+1})$ versus $(x - x_0)/\ell_0$ with the values of m given under method I in table 1 for each one of the three different turbulent flows. This figure should be compared with figure 3c which is a reproduction of figure 10 in Krogstad & Davidson (2011) where they plotted $< u_x^2 > \ell^3/(U^2\ell_0^3)$ versus $(x - x_0)/\ell_0$, except that we have offset the data vertically so as to see more clearly the differences in behavior between each grid. Assuming the turbulence is sufficiently homogeneous and isotropic and equally so for all three flows (as claimed by Krogstad & Davidson 2011), it is clear that the Saffman prediction is not satisfied in these flows. Instead,

$$u^2\ell^{m+1} = const \tag{2.4}$$

with $m > 2.5$ for all grids in the range $100\ell_0 \leqslant x - x_0 \leqslant 400\ell_0$. Furthermore, different grids give rise to different values of m reaching up to $m \approx 3$ with method I (see table 1).

In fact there is another way to extract values for n and m from the data (method II), and this way gives even better defined invariants and even greater differences between the far downstream turbulence decays originating from the conventional grid and the multiscale cross grids. Method II is based on figure 1b. This figure is a log-log plot of $Re_\lambda/Re_{\lambda 1}$ versus $(x - x_0)/l_0$ where $Re_{\lambda 1}$ is the value of Re_λ at the smallest distance from each grid on this plot and x_0 is the virtual origin obtained from our nonlinear fit of figure 1a. The first inescapable observation is that the streamwise distributions of Re_λ are clearly different for the conventional grid and for the multiscale grids.

The power law form (1.1) implies $\lambda^2 \sim (x - x_0)$ in decaying homogeneous isotropic turbulence (Batchelor (1953)). It follows that $Re_\lambda \sim (x - x_0)^{(1-n)/2}$, so that a best fit of the data in figure 1b gives values of n. We apply this power law fit to the very same range $80l_0 < x < 330l_0$ used in method I for our fit of the turbulence intensity data in figure 1a. The values of n thus obtained, the resulting values of m using (2.3) and the resulting $n_{corr} \equiv n/(1+p)$ are given in table 1 under method II. In figure 3b we use these new values of m to plot $< u_x^2 > \ell^{m+1}/(U^2\ell_0^{m+1})$ versus $(x - x_0)/\ell_0$ and find that they yield even better defined invariants (2.4) than method I (compare with figure 3a). The difference between values of m for conventional grids and values of m for multiscale grids is unmistakable and even greater with method II than with method I.

We must conclude that the decay of approximately homogeneous turbulence far from its initial conditions remains dependent on these initial conditions. The decay exponent n and the conserved finite invariant $u^2\ell^{m+1}$ both clearly change when the turbulence-generating grid is changed. These initial conditions may have to do with the geometry of the grids or/and with the inlet Reynolds numbers as the mean speed in the tunnel was $13.5m/s$ when the conventional grid was tested, $14.0m/s$ when *msg1* was tested and $15.5m/s$ when *msg2* was tested.

In trying to identify the flow-relevant geometrical variations from grid to grid, we note that the mustiscale grids of Krogstad & Davidson (2011) have three different bar widths $t_1 = 8mm$, $t_2 = 4mm$ and $t_3 = 2mm$ as well as three different mesh sizes $M_1 = 2M_2$ and $M_2 \approx 2M_3$ with $M_1 = 64mm$ in the case of *msg1* and $M_1 = 88mm$ in the case of *msg2*

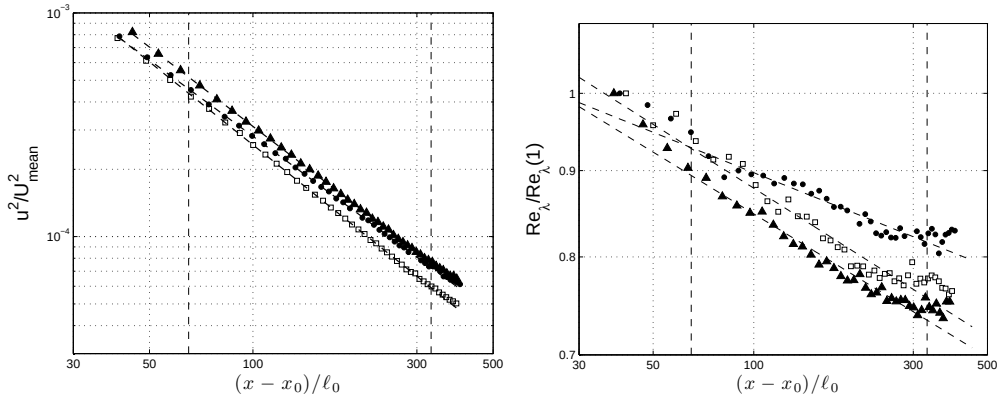

FIGURE 1. Data and best-fit power laws for: (a) $< u_x^2 > /U_{mean}^2$ versus $(x-x_0)/\ell_0$ (b) $Re_\lambda/Re_{\lambda 1}$ versus $(x-x_0)/\ell_0$. (●) *cg*, (▲) *msg1*, (□) *msg2*. The vertical dashed lines mark the start and end of the admissible data range used in the least-squares fits.

TABLE 1. Estimation of quantities via least squares fit

		Method I					Method II			
Grid	p	n	x_0(m)	m	n_{corr}	α	n	m	n_{corr}	α
cg	0.126	1.13	0.23	2.67	1.29	1.90	1.15	2.85	1.32	1.68
msg1	0.101	1.18	0.28	2.79	1.31	1.14	1.24	3.38	1.37	0.86
msg2	0.072	1.23	0.33	2.94	1.33	0.62	1.25	3.14	1.35	0.57

(see their figure 1). Hence the ratio of mesh size to bar width is 11 for *msg2* and 8 for *msg1*. It is therefore at least double than $M/t = 4$ for the conventional grid *cg*.

The mesh size determines the distance between the wakes of the bars and the bar thickness determines the width of these wakes. Hence the ratio of mesh size to bar thickness determines the distance from the grid where the wakes meet and this distance increases when we move from *cg* to *msg1* and *msg2*.

The Reynolds numbers characterising these wakes (calculated as the mean flow speed multiplied by the bar thickness and divided by the kinematic viscosity of the air) take the values 3.6×10^3 in the case of *cg*; 3×10^3, 1.5×10^3 and 7.5×10^2 in the case of *msg1*; and 3.32×10^3, 1.66×10^3 and 8.3×10^2 in the case of *msg2*. Unlike conventional grids, multiscale grids impose more than one Reynolds number on the flows they generate and a number of different distances from the grid where wakes of different sizes meet. Of course the largest wakes are affected by the wakes generated by the smaller ones. But it is clear that the turbulence undergoes different generation mechanisms extending over different streamwise distances with different grids. It is indeed remarkable that memory of these mechanisms remains in the values of n and m as far downstream as where Krogstad & Davidson (2011) took their measurements.

3. Different far-field low-Re_λ turbulent flows

We obtained figures 3a,b by taking into account the slow streamwise variation of A as suggested by Krogstad & Davidson (2010). This streamwise variation can result from the

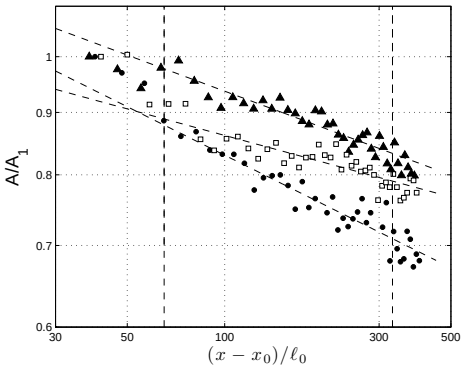

FIGURE 2. Data and best-fit power laws for A/A_1 versus $(x - x_0)/\ell_0$. (●) *cg*, (▲) *msg1*, (□) *msg2*. The vertical dashed lines mark the start and end of the admissible data range used in the least-squares fits.

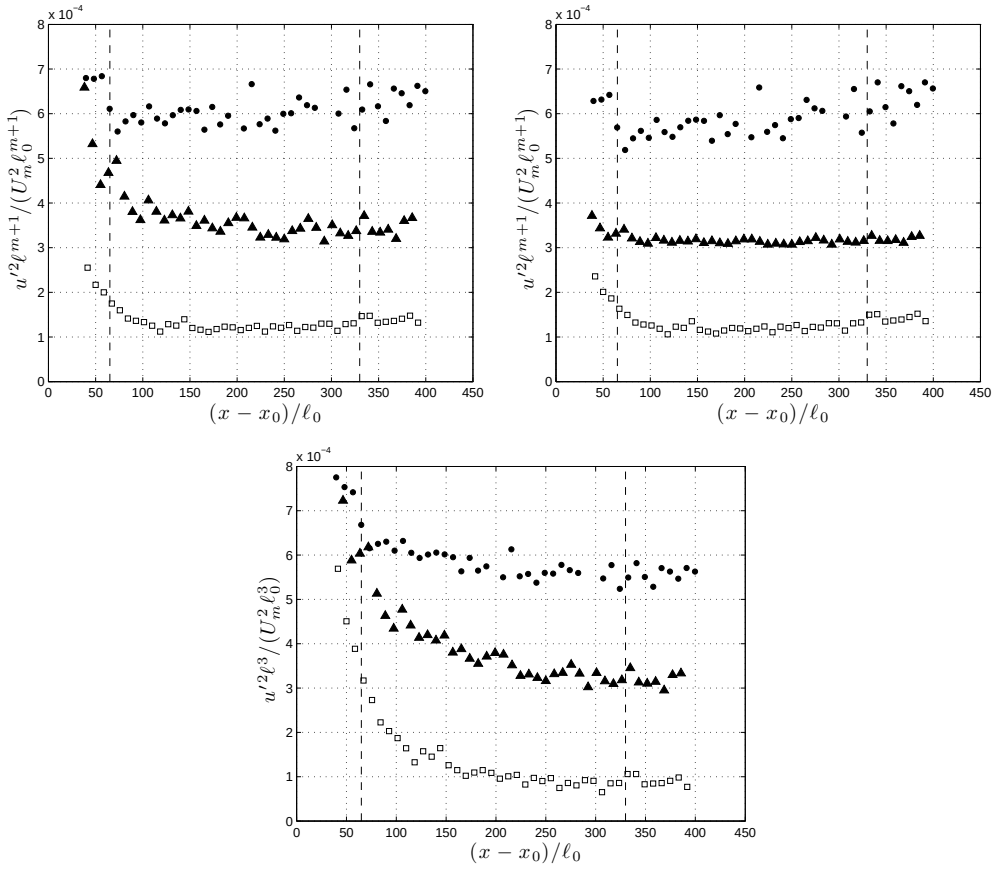

FIGURE 3. Checks of invariant forms via plots of $u^2\ell^{m+1}$: (a) m from method I, (b) m from method II, (c) $m = 2$ corresponding to Saffman turbulence. (●) *cg*, (▲) *msg1*, (□) *msg2*. For improved readability the *cg*/*msg1*/*msg2* data were vertically offset by (a) $[2.0,\ 1.0,\ 0.0] \times 10^{-4}$, (b) $[1.6,\ 2.5,\ 0.0] \times 10^{-4}$, (c) $[2.5,\ 0.5,\ -1.5] \times 10^{-4}$.The left and right vertical dashed lines mark the start and end of the data range used to obtain the decay exponents n. This is the range not significantly affected by inhomogeneity (to the left) and noise (to the right).

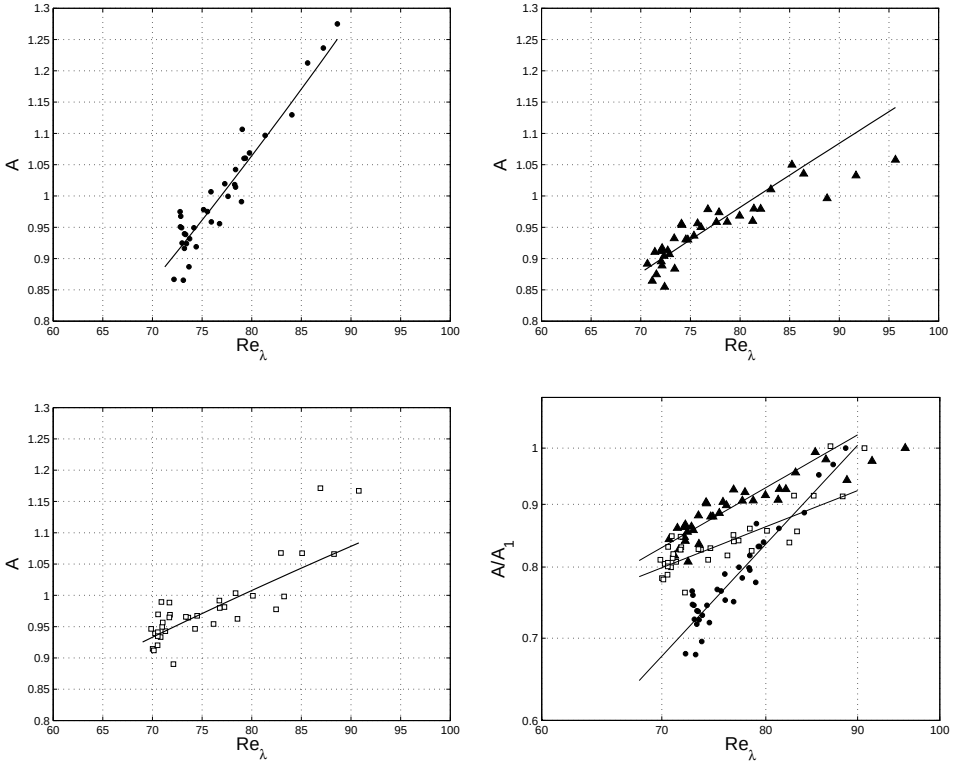

FIGURE 4. Re_λ dependence of the normalised energy dissipation rate A (note that A here is $3A/2$ in Krogstad & Davidson (2011), for example see their figure 11): (a) *cg*, (b) *msg1*, (c) *msg2*, (d) logarithmic axes. (●) *cg*, (▲) *msg1*, (□) *msg2*. The solid lines are plots of $A = const \times Re_\lambda^\alpha$ with α taken from table 1, method II.

well-known dependence that the dimensionless dissipation rate A has on Re_λ when Re_λ is below at least 100 (e.g. Burattini, Lavoie & Antonia 2005). Indeed, the values of Re_λ characterising the three far-field turbulent flows of Krogstad & Davidson (2011) range between about 90 near $x \approx 60\ell_0$ and 70 at $x \approx 330\ell_0$. Using $Re_\lambda \sim (x - x_0)^{(1-n)/2}$ and $A \sim (x - x_0)^{-p}$ we obtain

$$A \sim Re_\lambda^\alpha \tag{3.1}$$

where

$$\alpha = 2p/(n-1). \tag{3.2}$$

The values of α implied by this formula on the basis of the exponents p and n obtained in the previous section are very different for different grids, ranging from $\alpha \approx 1.7$ to $\alpha \approx 0.6$ (using n obtained from method II, see table 1). Figure 4 confirms how dramatically different the dependencies of A on Re_λ are for the multiscale grids and for the conventional grid. Hence, multiscale grids definitely do not "produce almost identical results to the equivalent classical grids" as claimed by Krogstad & Davidson (2011).

Figure 4 also shows that (3.1)-(3.2) give rise to more or less reasonable fits of the data thus lending support to the idea that much of the streamwise variation of A comes from its dependence on Re_λ. Increasing values of the dimensionless dissipation rate A with increasing Re_λ have also been reported in previous works with square bar grids at such

relatively low Reynolds numbers, see for example figure 1 in Burattini *et al.* (2005), table 4 in Comte-Bellot & Corrsin (1971) and table 3 in Gad-El-Hak & Corrsin (1974).

4. Conclusion

According to the published data in Krogstad & Davidson (2011), multiscale cross grids and their equivalent (in terms of ℓ_0) conventional grid can produce very different far-field approximately homogeneous isotropic turbulence with wide variations in the dimensionless dissipation rate's dependence on Re_λ. This would seem to confirm the observation already made by Burattini *et al.* (2005) on the basis of different Re_λ dependencies of A for different grids, namely that "the geometry of the grid appears to have a persistent influence in the streamwise direction up to $x/M = 80$". In fact the data of Krogstad & Davidson (2011) extend this observation to much further distances downstream and to a wider range of grids.

This data also leads to the conclusion that the decay of the three approximately homogeneous isotropic turbulent flows of Krogstad & Davidson (2011) is characterised by an invariant quantity $u^2\ell^{m+1}$ in the region of the flow $x \geqslant 80\ell_0$ which is the most clearly homogeneous. The exponent m is significantly different from Saffman's $m = 2$ and ranges between 2.7 and 3.4 for the grids used by Krogstad & Davidson (2011). Their multiscale grids return values of m which are markedly larger than the values of m returned by their conventional grid. The streamwise distributions of Re_λ and A are also very clearly different.

Finally we repeat the remark in our introduction that the data of Krogstad & Davidson (2011) do not contradict previous findings on multiscale grids but in fact complement them.

We thank Professor Per-Åge Krogstad for kindly providing us with the post-processed data published in Krogstad & Davidson (2011).

REFERENCES

Batchelor, GK & Townsend, AA 1948 Decay of isotropic turbulence in the initial period. *Proceedings of the Royal Society of London. Series A, Mathematical and Physical Sciences* **193** (1035), 539–558.

Batchelor, G. K. 1953 *The theory of homogeneous turbulence*. Cambridge University Press, Cambridge.

Burattini, P., Lavoie, P. & Antonia, R.A. 2005 On the normalized turbulent energy dissipation rate. *Physics of Fluids* **17**, 098103.

Comte-Bellot, G. & Corrsin, S. 1971 Simple Eulerian time correlation of full-and narrow-band velocity signals in grid-generated, isotropic turbulence. *J. Fluid Mech.* **48** (02), 273–337.

Gad-El-Hak, M. & Corrsin, S. 1974 Measurements of the nearly isotropic turbulence behind a uniform jet grid. *J. Fluid Mech.* **62** (01), 115–143.

Geipel, P., Henry Goh, K. H. & Lindstedt, R. P. 2010 Fractal-generated turbulence in opposed jet flows. *Flow Turbulence Combust.* **85** (3–4), 397–419.

George, W. K. 1992 The decay of homogeneous isotropic turbulence. *Physics of Fluids A* **4** (7), 1492–1509.

Hurst, D. J. & Vassilicos, J. C. 2007 Scalings and decay of fractal-generated turbulence. *Physics of Fluids* **19**, 035103.

Kinzel, M., Wolf, M., Holzner, M., Lüthi, B., Tropea, C. & Kinzelbach, W. 2010 Simultaneous two-scale 3D-PTV measurements in turbulence under the influence of system rotation. *Exp Fluids* (to appear).

Krogstad, P. Å. & Davidson, P. A. 2010 Is grid turbulence Saffman turbulence? *J. Fluid Mech.* **642**, pp 373–394.

Krogstad, P. Å. & Davidson, P. A. 2011 Freely decaying, homogenous turbulence generated by multi-scale grids. *J. Fluid Mech.* (to appear).

Laizet, S. & Vassilicos, J. C. 2011 DNS of fractal-generated turbulence. *Flow Turbulence Combust.* (to appear).

Lavoie, P., Djenidi, L. & Antonia, R.A. 2007 Effects of initial conditions in decaying turbulence generated by passive grids. *J. Fluid Mech.* **585**, 395–420.

Mazellier, N. & Vassilicos, J. C. 2010 Turbulence without Richardson-Kolmogorov cascade. *Physics of Fluids* **22**, 075101.

Nagata, K., Suzuki, H., Sakai, Y., Hayase, T. & Kubo, T. 2008*a* Direct numerical simulation of turbulent mixing in grid-generated turbulence. *Physica Scripta* **2008**, 014054.

Nagata, K., Suzuki, H., Sakai, Y., Hayase, T. & Kubo, T. 2008*b* DNS of passive scalar field with mean gradient in fractal-generated turbulence. *Int. Rev. Phys* **2**, 400.

Rotta, J. C. 1972 *Turbulente Strömungen: eine Einführung in die Theorie und ihre Anwendung*. B.G. Teubner, Stuttgart.

Seoud, R. E. & Vassilicos, J. C. 2007 Dissipation and decay of fractal-generated turbulence. *Physics of Fluids* **19**, 105108.

Stresing, R., Peinke, J., Seoud, R. E. & Vassilicos, J. C. 2010 Defining a new class of turbulent flows. *Phy. Rev. Lett.* **104** (19), 194501.

Suzuki, H., Nagata, K., Sakai, Y. & Ryota, U. 2010 High-Schmidt-number scalar transfer in regular and fractal grid turbulence. *Physica Scripta* **2010**, 014069.

Valente, P. C. & Vassilicos, J. C. 2011 The decay of homogeneous turbulence generated by a class of multi-scale grids. *Under Consideration for J. Fluid Mech.* ArXiv:1101.0709v1.

Vassilicos, J. C. 2011 An infinity of possible invariants for decaying homogeneous turbulence. *Physics Letters A* **375** (6), 1010 – 1013.